Initial Off-axis Beam Experiments in DIII-D

M.A. Van Zeeland[1], W.W. Heidbrink[2], J.M. Park[3], R. Prater[1], C.T. Holcomb[4], M.E. Austin[5], J.R. Ferron[1], C.M. Greenfield[1], B.A. Grierson[6], R.-M. Hong[1], T.C. Luce[1], G.R. McKee[7], R.A. Moyer[8], M. Murakami[3], C.J. Murphy[1], C.M. Muscatello[2], D.C. Pace[1], C.C. Petty[1], J. Rauch[1], J.T. Scoville[1], W.M. Solomon[6], and B.J. Tobias[6]

[1]*General Atomics, PO Box 85608, San Diego, California 92186-5608, USA*
[2]*University of California, Irvine, Irvine, California 92697 USA*
[3]*Oak Ridge National Laboratory, PO Box 2008, Oak Ridge, Tennessee 37831, USA*
[4]*Lawrence Livermore National Laboratory, Livermore, California 94550, USA*
[5]*University of Texas at Austin, Austin, Texas 78712-1047, USA*
[6]*Princeton Plasma Physics Laboratory, Princeton, New Jersey 08543-0451, USA*
[7]*University of Wisconsin-Madison, Madison, Wisconsin 53706, USA*
[8]*University of California San Diego, La Jolla, California 92093-0417, USA*

To realize steady-state high performance discharges in ITER and future tokamaks, 100% of the current must come from noninductive sources such as bootstrap current, electron cyclotron current drive, and neutral beam current drive (NBCD). Experimentally, such high-performance noninductive discharges have been demonstrated in DIII-D; however, the duration is usually limited by the evolution of the current profile to an unstable state. Experimental measurements and simulations of these discharges have indicated that they could be extended to near steady state if the current profile were maintained by replacing the remaining Ohmic current with NBCD near the half-radius [1]. In support of this goal, one of DIII-D's beamlines was modified to allow adjustable off-axis injection and current drive. This paper discusses the neutral beam modification, initial experiments to assess basic beam functionality as well as driven current, and initial physics experiments in which the new off-axis beam was used to vary Alfvén eigenmode (AE) stability.

DIII-D is equipped with four neutral beamlines (30, 150, 210 and 330 — toroidal angle location), all of which inject horizontally from outside midplane ports and contain two separate sources (R and L). Three of the beamlines 30, 150, and 330 are oriented to inject in the same direction as the standard plasma current direction ("co-injection") while the fourth beamline 210, was reoriented in 2006 to inject in the counter direction. Three co-injection beamlines provide considerable co-current drive while the counter beamline drives current in the counter direction. In both cases, the current is predominantly driven near the plasma axis since the beamlines are aimed along the midplane and beam ion density is typically highest in the central region of the plasma. In 2011, the 150 co-injection neutral beamline was modified to provide off-axis current drive.

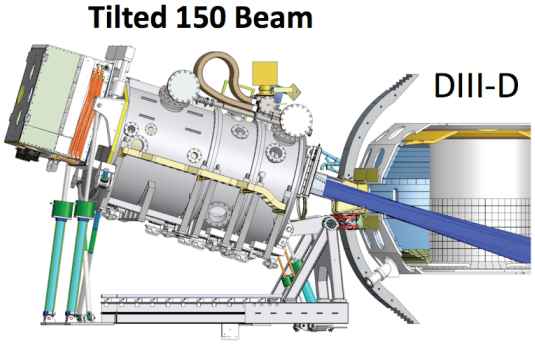

Fig. 1. Engineering model showing the tilted 150 beam and injected neutral path (blue).

Injection of the 150 beams off-axis at mid-radius (target values, 150R $\delta z \approx$ -35 cm and 150L $\delta z \approx$-40 cm at R=1.7 m,) required a combination of both beamline vertical tilt and ion

source tilt [2]. Tilting of the 150 beam (OANB) was limited to a maximum of 16.5 deg and was accomplished using a single large front hydraulic cylinder and two rear hydraulic cylinders. Figure 1 shows an engineering drawing of the tilted beam and its injection trajectory into DIII-D.

Initial experiments were carried out with the goal of assessing basic OANB performance, characterizing the beam, verifying the steering, deposition, and developing models. Figure 1(a-c) show fast framing camera images of D_α emission during beam into neutral deuterium gas injection [3] at a range of beam and source tilts. These images yield the beam vertical profile as well as verify beam trajectories relative to design values. With no beam or source tilt, the 150 beamline functions as the other on-axis co-sources. As the beam and source are tilted, the centerline trajectory moves lower as expected. From Fig. 2(c), it is clear that with the beam and source tilt at 16.4 deg. and 35 minutes respectively, the beam centerline achieves the design target. Also apparent in Fig. 2(c) is a small amount of clipping that occurs on the lower portion of the beam. The clipped beam particles are lost to both internal collimators and the port box. In the maximum tilted position, this results in an additional ≈4% loss in beam power relative to the untilted position. Figure 2(d) shows the results of TRANSP/NUBEAM [4] modeling for the configuration of Figure 2(c) with the source geometry taken from engineering drawings (each beam is described by four individual sources) and a vertical divergence adjusted to match the experimental beam profiles. The TRANSP/NUBEAM model reproduces well the measured vertical beam profile, steering, and clipping throughout the entire tilt range.

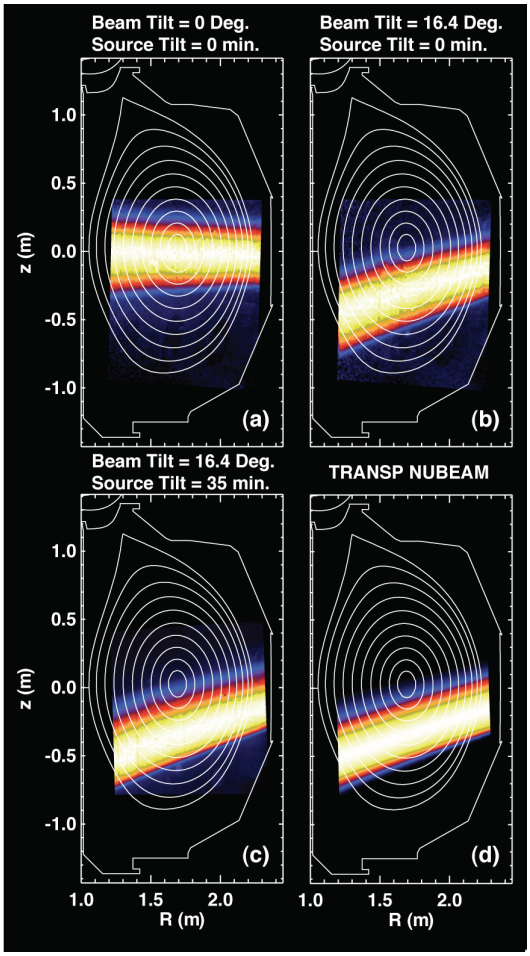

Fig. 2. (a-c) D_α images of 150R beam into neutral deuterium gas at different beam and source tilts. Note, images are normalized at each vertical column of pixels to remove intensity reduction due to attenuation. (d) TRANSP modeling of figure (c). Equilibrium flux surfaces are shown only for reference.

Radially resolved measurements of the confined fast ion profile during OANB injection were made using DIII-D's fast ion D_α (FIDA) system [5] as well as main ion D_α spectrometer system [6]. The main ion system allows fits to the entire D_α spectrum including thermal charge exchange, injected neutral emission, and fast ion charge exchange or FIDA and provides excellent radial profile measurements of the region of phase space populated by the OANB ions.

Figure 3 shows the FIDA emission profile during two different time periods immediately following on-axis (black) and off-axis (red) injection. These data confirm the expected shift away from the magnetic axis for off-axis injection and a hollow FIDA emission profile. Comparison to modeling, however, shows that the magnitude of the measured brightness is lower than predicted for the off-axis beams by up to 30%, analysis of which is ongoing [7].

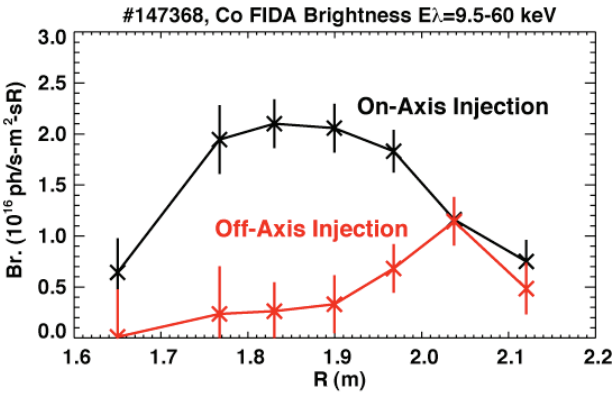

Fig. 3. FIDA brightness for DIII-D discharge 147368 from main ion D-alpha system. Black curve during on-axis beam injection (P=2.23 MW) and red during off-axis injection (P=1.87 MW).

The OANB driven current was evaluated using a pair of H-mode discharges with on and off-axis injection and matched profiles of electron temperature and density. By matching discharge parameters and comparing purely on-axis to off-axis injection, we reduce our susceptibility to model dependencies and systematic uncertainties of the various measurements. The motional Stark effect (MSE) polarimeter measured equilibrium pitch angles at various radii for two discharges with matched conditions, varying only by the use of on/off axis beams after t=1.2 s, are shown in Fig. 4(a). The MSE data show a clear change in pitch angle due to the switch from on to off-axis beam injection with the largest changes in the core. These results are compared to NUBEAM modeling in Fig. 4(b), where the radial profiles of beam driven current are shown. Beam driven current is evaluated by subtracting the Ohmic and bootstrap current from the total current obtained using the MSE constrained kinetic equilibrium reconstructions [8]. The Ohmic current is derived using the neoclassical conductivity and internal loop voltage from a series of equilibrium reconstructions and the bootstrap current is obtained from neoclassical theory and equilibrium profiles. The NBCD profiles show the expected shift from centrally peaked for on-axis injection to peaked near mid-radius for off-axis injection. The magnitude and shape of the beam driven current are consistent with NUBEAM modeling. Off-axis NBCD variation for a range of conditions, including toroidal field direction, beam injection power, plasma beta (β), and ratio of beam

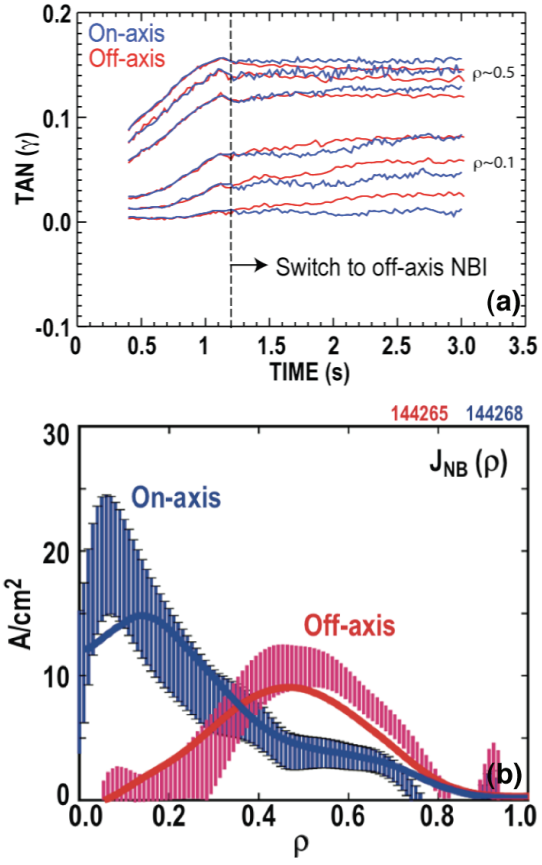

Fig. 4. (a) MSE measured pitch angles vs. time at different radii for on-axis injection (144268) and switching to off-axis injection after t=1.2 s (144265). (b) Radial profiles of NBCD. Measurements with error bars are given and solid thin curves are NUBEAM modeling.

injection energy to electron temperature (E_b/T_e), will be presented in future publications [9]. Also, first steps in the application of off-axis NBCD to steady-state high-performance scenarios show that the off-axis capability enables operation at higher minimum safety factor with broader pressure profiles than previously obtainable in DIII-D [10].

In addition to NBCD studies and furthering the goal of 100% noninductive discharges, DIII-D's new off-axis beam capability provides a unique tool for studying fundamental aspects of fast ion physics. One specific example is the use of the OANB to vary the fast ion pressure profile and the drive for EP instabilities such as AEs. In DIII-D, AEs driven by the fast beam ions are commonly observed during the current ramp portion of discharges with early beam heating [11]. Initial experiments took advantage of the OANB to vary the fast ion pressure gradient ($\nabla\beta_f$) in the vicinity of reversed shear AEs (RSAEs) near q_{min}. Systematic scans from on-axis to off-axis injection in a series of discharges determined the stability and impact on RSAEs and toroidicity induced AEs (TAEs) as $\nabla\beta_f$ was varied. The results of this scan are shown in Fig. 5 where spectrograms of ECE data during on-axis and off-axis injection are shown for two different radii. Consistent with the so-called "standard drive" mechanism, these data show the AE stability is significantly altered by off-axis injection, with RSAEs disappearing in regions where the fast ion gradient is weakened [Fig. 5(a) and Fig. 5(c)]. TAEs remain unstable at larger radius where gradients are expected to be similar to those from on-axis injection [Fig. 5(b) and Fig. 5(d)]. Future work will compare detailed gyrokinetic calculations of the eigenmode stability with the observed mode spectra during OANB injection.

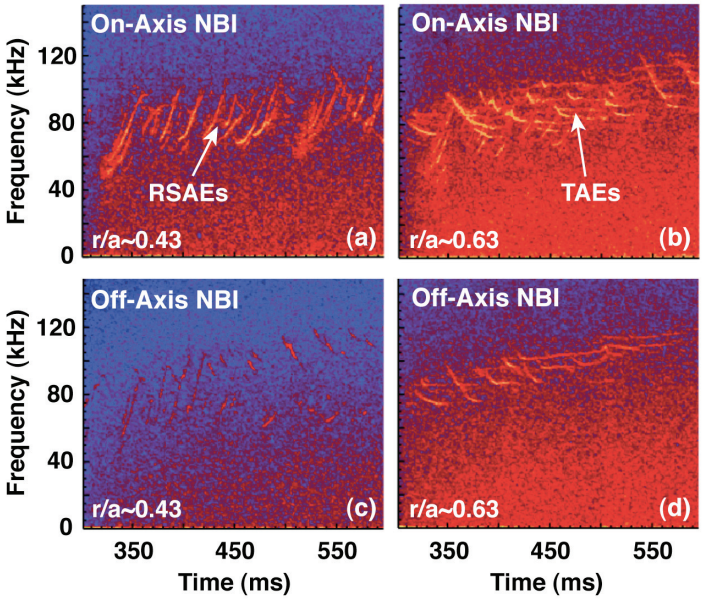

Fig. 5. ECE spectrograms at two different radii (r/a~0.43 and r/a~0.63) for DIII-D discharge #146076 on-axis injection (a,b), and #146077 off-axis injection (c,d).

This work was supported by the US Department of Energy under DE-FC02-04ER54698, SCG903402, DE-AC05-00OR22725, DE-AC52-07NA27344, DE-FG03-97ER54415, DE-AC02-09CH11466, DEFG02-89ER53296, DE-FG03-08ER54999, and DE-FG02-07ER54917.

[1] M. Murakami, *et al.,* Nucl. Fusion **49**, 065031 (2009).
[2] C. Murphy, *et al.,* Proc. 24th Symp. on Fusion Engineering, Chicago, IL (2011).
[3] M.A. Van Zeeland, *et al.,* Plasma Phys. Control. Fusion **52**, 045006 (2010).
[4] A. Pankin, *et al.,* Comp. Phys. Comm. **159**, 3 (2004).
[5] W.W. Heidbrink, *et al.,* Plasma Phys. Control. Fusion **46**, 1855 (2004).
[6] B.A. Grierson, Phys. Plasmas **19**, 056107 (2012).
[7] W.W. Heidbrink, *et al.,* Nucl. Fusion, *In Press* (2012).
[8] J.M. Park, *et al.,* Phys. Plasmas **16**, 092508 (2009).
[9] J.M. Park, *et al.,* IAEA-FEC, San Diego, CA (2012).
[10] C.M. Holcomb, *et al.,* IAEA-FEC, San Diego, CA (2012).
[11] W.W. Heidbrink *et al.,* Phys. Plasmas **15**, 055501 (2008).